Rapid flip-flop motions of diacylglycerol and ceramide in phospholipid bilayers

Fumiko Ogushi [a], Reiko Ishitsuka [b], Toshihide Kobayashi [b], Yuji Sugita [a,c,d,*]

[a] Theoretical Biochemistry Laboratory, RIKEN Advanced Science Institute, 2-1 Hirosawa, Wako-shi, Saitama 351-0198, Japan
[b] Lipid Biology Laboratory, RIKEN Advanced Science Institute, 2-1 Hirosawa, Wako-shi, Saitama 351-0198, Japan
[c] Computational Biophysics Research Team, RIKEN Advanced Institute for Computational Science, 7-1-26 Minatojimaminamimachi, Chuo-ku, Kobe 650-0047, Japan
[d] Laboratory for Biomolecular Function Simulation, RIKEN Quantitative Biology Center, 7-1-26 Minatojimaminamimachi, Chuo-ku, Kobe 650-0047, Japan

ARTICLE INFO

ABSTRACT

We have investigated flip-flop motions of diacylglycerol and ceramide in phospholipid bilayers using coarse-grained molecular dynamics simulations. In the simulations, flip-flop motions of diacylglycerol and ceramide in the DAPC membrane are slower than cholesterol. Rates correlate with the number of unsaturated bonds in the membrane phospholipids and hence with fluidity of membranes. These findings qualitatively agree with corresponding experimental data. Statistical analysis of the trajectories suggests that flip-flop can be approximated as a Poisson process. The rate of the transverse movement is influenced by depth of the polar head group in the membrane and extent of interaction with water.

© 2011 Elsevier B.V. All rights reserved.

1. Introduction

Lipid molecules are heterogeneously distributed in biological membranes according to region and situation [1]. Selective distribution is achieved through fast or slow diffusion along or across membranes. The transverse diffusion between bilayer leaflets (flip-flop motion) is fundamental to the lipid distribution and the membrane dynamics. Flip-flop motion occurs in several ways. The spontaneous flip-flop motions of phosphatidylcholine (PC) type lipids are very slow and are associated with water entry into hydrophilic regions of the membrane. This water-mediated flip-flop process of PC lipids has been studied not only by experiments but also by theoretical simulations [2]. Specific membrane proteins (flippase and sclambrase) greatly speed up the transverse motion of these PC type lipids [3]. On the other hand, biological second messenger lipids like diacylglycerol (DAG) or ceramide (CER) are important example to mediate rapid lipid trafficking. These lipids undergo rapid spontaneous flip-flop motions without the assistance of membrane proteins or the formation of the membrane pore and play a role in the heterogeneous distribution of lipid molecules and in increasing membrane flexibility [4].

Diacylglycerol (DAG) and ceramide (CER) are central intermediates in the biosynthesis and degradation of eukaryotic lipids as well as being major lipid second messengers [5]. DAG is synthesized de novo by the acylation of monoacylglycerol. Further acylation produces triacylglycerol, which is a major storage lipid of cells,

whereas the addition of a hydrophilic head group results in phospholipids and glycoglycerolipids that form cellular membranes [6]. Lipase-mediated catabolism of triacylglycerol and phospholipase-dependent degradation of phospholipids result in the production of DAG. It is well established that phospholipase-C mediated generation of DAG activates the protein kinase C cascade [7–9]. CER is an intermediate in the de novo synthesis of all sphingolipids. In mammalian cells, CER is synthesized on the cytoplasmic side of the endoplasmic reticulum and then transported to the Golgi apparatus. CER is metabolized to sphingomyelin (SM) in the Golgi lumen whereas conversion of CER to glucosylceramide occurs on the cytoplasmic side of the organelle [10,11]. The degradation of cell-surface SM to CER by the activation of sphingomyelinase induces the formation of specific CER-rich lipid domains, which provides a signaling platform for events as diverse as apoptosis and differentiation [12].

Since the precise cellular localization of DAG and CER determines their fate and activity, it is important to understand their distribution and dynamics. Information on transbilayer movement is crucial to an understanding of metabolism and signaling involving DAG and CER. Fluorescent and spin-labeled lipid analogs have been used to study the dynamics of DAG and CER. Using lipid analogs labeled with the fluorescent fatty acid, 5-(5,7-dimethyl BODIPY)-1-pentanoic acid (C_5–DMB–), Bai and Pagano showed that C_5–DMB–CER and C_5–DMB–DAG exhibit rapid spontaneous transbilayer movement [13], while C_5–DMB–SM and C_5–DMB–PC move across the bilayer very slowly. Rapid transbilayer movement has been also observed using sulfhydryl analogs of DAG [14]. Little is known about the transbilayer movement of naturally occurring DAG and CER because of technical difficulties.

In this Letter, we investigated flip-flop motions of DAG and CER using computer simulations as research tools. The dynamic

---

* Corresponding author at: Theoretical Biochemistry Laboratory, RIKEN Advanced Science Institute, 2-1 Hirosawa, Wako-shi, Saitama 351-0198, Japan. Fax: +81 48 467 4532.
E-mail addresses: f_ogushi@riken.jp (F. Ogushi), isitsuka@riken.jp (R. Ishitsuka), kobayasi@riken.jp (T. Kobayashi), sugita@riken.jp (Y. Sugita).

properties of lipid-bilayer systems have previously been examined using atomistic MD simulations in conjunction with experiments [15–22]. However, due to the slow time-scale of flip-flop motions for most lipid molecules during the time scale of the simulations, we employed the MARTINI coarse-grained (CG) model in most of our MD simulations [23,24]. The model unites approximately four atoms into a CG particle, resulting in a 200-fold saving of computational time compared with atomistic MD simulations while reproducing structural, dynamic, and thermodynamic properties of membranes on a semi-quantitative level [23]. We carried out CGMD simulations of DAG and CER for approximately 80 μs in three PC bilayer systems with different degrees of fatty acid unsaturation. For comparison, we also performed CGMD simulations of cholesterol (CHOL) in the same PC bilayer systems, these having been already investigated by Marrink et al. [18]. In the simulations, we reproduced the experimental order of flip-flop rates for CHOL, DAG, and CER. We also examined the mechanism that determines these rates in different PC bilayer systems, using CGMD and atomistic MD simulations.

2. Methods

2.1. System description

We constructed nine simulation systems, in which CHOL, 1-palmitoyl-2-oleoyl-*sn*-glycerol (PODAG, 16:0–18:1 DAG), or C18 ceramide (SCER, *N*-stearoyl-D-*erythro*-sphingosine) (see Figure 1) are embedded in three different phospholipid bilayers like 1-palmitoyl-2-oleoyl-*sn*-glycero-3-phosphocholine (POPC, 16:0–18:1 PC), 1-stearoyl-2-arachidonoyl-*sn*-glycero-3-phosphocholine (SAPC, 18:0–20:4 PC), and 1,2-di-arachidonoyl-*sn*-glycero-3-phosphocholine (DAPC, di20:4 PC). In this Letter, these mixed bilayer systems are referred to as CHOL/POPC, CHOL/SAPC, CHOL/DAPC, and so on. In modeling these systems, we started with PC bilayer systems containing 42 POPC, SAPC, or DAPC molecules and replaced four of the molecules with CHOL, PODAG, or SCER, which were selected randomly. Thus, CHOL, PODAG, or SCER made up 10% of each phospholipid bilayer.

We used MARTINI coarse-grained (CG) models in our MD simulations to investigate flip-flop motions of CHOL, PODAG, and SCER [23,24]. Recently, MARTINI models have been widely used in simulations of membranes or other biological systems and have been shown to reproduce their structural and dynamic properties qualitatively [23]. We used MARTINI models for POPC, SAPC, DAPC, CHOL, and the CG water in the GROMACS software package [25–27]. We made models for SCER and PODAG, combining the MARTINI CG particles (Figure 1). The CG models of these two lipids are illustrated with colored circles. The hydroxyl head group of each lipid is mapped into one CG bead (shown in white for DAG and CER). The glycerol backbone (GL) and sphingo backbone are mapped into two CG beads (shown in green for DAG and purple for CER). Acyl tails, palmitoyl, oleoyl, and steoyl are mapped into four or five beads (shown in cyan). To examine the effect of the interaction between water and lipid molecules, we performed 80 μs CGMD simulations for DAPC mixed lipid-bilayer systems using the polarizable MARTINI water model [28]. These systems contain 152 DAPC and 2400 water molecules and the same concentrations of mixed lipid molecules (CHOL. SCER, or PODAG).

We also performed atomistic MD simulations for CHOL/DAPC, PODAG/DAPC, and SCER/DAPC to investigate the interaction of water molecules at the membrane/water interfaces. The starting conformations of atomistic MD simulations were obtained from the final snapshots in the CGMD simulations of the same systems. After removing the CG water particles, all the CG particles in the lipid molecules are mapped to the atomistic models, using the
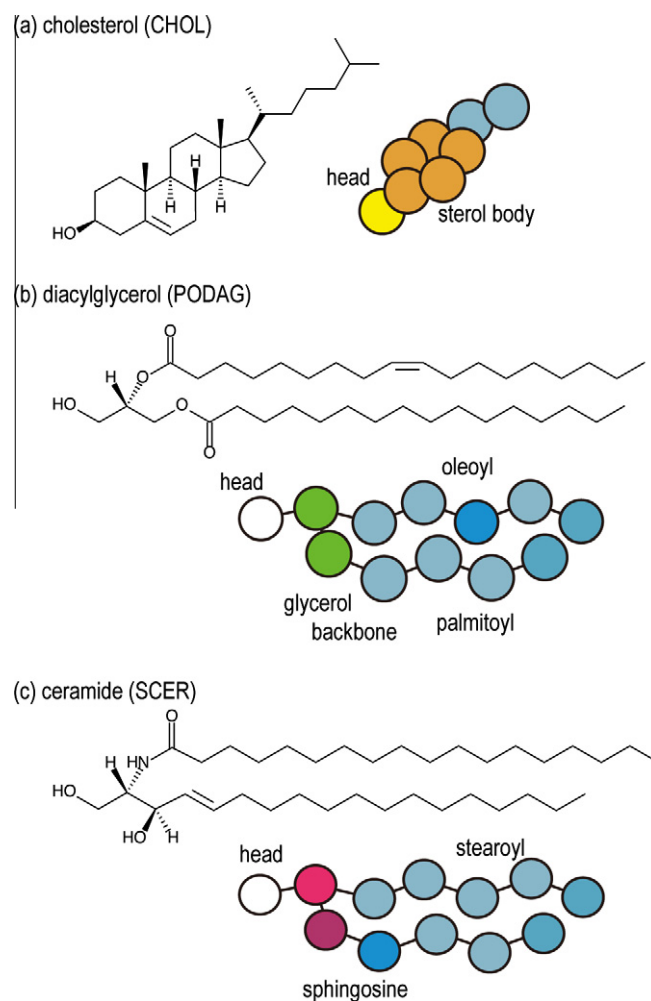
Figure 1. Chemical structures and MARTINI coarse-grained models for (a) cholesterol (CHOL), (b) 1-palmitoyl-2-oleoyl-*sn*-glycerol (PODAG), and (c) C18 ceramide (SCER) are illustrated. Each color of a CG particle represents a different particle type in the MARTINI CG models.

g_fg2cg program in GROMACS software package. In the CG and atomistic MD simulations, we filled 600 CG water particles and 2400 water molecules, respectively. The force field parameters developed by Berger et al. were employed for DAPC, CHOL, PODAG, and SCER [29–31]. A simple-point charge (SPC) model was used for water molecules [32]. When original parameters for lipid molecules are not found in the GROMACS parameter files, we took parameters from the same chemical groups in different lipid molecules [33–35].

2.2. Simulation procedures

In CG and atomistic MD simulations, we used the GROMACS simulation package [25–27]. Before starting MD simulations, we carried out an energy minimization for 1000 steps to relax each simulation system.

The standard treatment of nonbonded interactions for the MARTINI models was employed (r_{cut} = 1.2 nm and r_{shift} = from 0.9 nm to r_{cut}) [23,24,36]. A rectangular parallel piped box with a periodic boundary condition was applied to each system. Each molecule was separately coupled with a heat bath at 300 K and a relaxation time of t_T = 0.1 ps. The relaxation time of t_P = 0.5 ps was used for the semi-isotropic pressure coupling where lateral (*x–y* plane) and bilayer normal (*z*-axis) directions were separately controlled.

In the systems containing CHOL, we used an integration time step of 30 fs and an update of the neighboring list every 10 steps, whereas in other systems, we used a time step of 40 fs with the same update frequency. The systems containing CHOL (CHOL/DAPC, CHOL/SAPC, and CHOL/POPC) were simulated for 67×10^7 steps, whereas other systems were simulated for 50×10^7 steps. Due to the smoothness of CG potential energy surfaces, the dynamics of the CG particles is faster than the atomistic motions in all-atom model MD simulations.

Time-scale in CG models is carefully treated in each MD simulation. Conventionally, a factor of four is used in simulations based on the MARTINI coarse-grained model. This factor is determined by comparing the diffusion constant of CG water molecules at 300 K with experimental measurements. However the factor may be different in different molecular systems. To check this, we compared the lateral diffusion constants of CHOL, PODAG, and SCER in a DAPC membrane. The results (Table 2 in Supporting Information) show that the factor ranges from 2 to 7 in a DAPC mixed bilayer. For convenience of comparison with preceding studies using MARTINI models, hereafter, we use four as the standard conversion factor to obtain an effective time scale [24]. The total (effective) simulation times for the systems containing CHOL (CHOL/DAPC, CHOL/SAPC, and CHOL/POPC) were 80.4 μs and other systems were simulated for 80 μs.

In the atomistic simulations for CHOL/DAPC, PODAG/DAPC, and SCER/DAPC, Lennard–Jones and Coulombic interactions were cut off at 0.9 nm. The smooth particle mesh Ewald method was used for long-range electrostatic interactions [37,38]. Bond lengths were constrained with the LINCS algorithm [39] for lipid molecules, and with the SETTLE algorithm for water molecules [40], allowing an integration time step of 2 fs. The temperature and pressure of transverse lipid, PC lipid, and water molecule were set to 300 K and 1 bar using Berendsen's algorithm [41] with coupling constants of 0.1 ps and 2.5 ps, respectively. After 10 ns equilibration, we performed 100 ns atomistic MD simulation for each system for production dynamics.

3. Results and discussion

3.1. Structural properties of the mixed bilayer systems

Table 1 lists the structural properties of the nine lipid bilayers in the CGMD simulations. Bilayer thickness ($\Delta Z/2$) is defined as the distance between the average positions of GL of PC in upper and lower leaflets. We define area per lipid (A) as the cell area parallel to the membrane divided by the total number of lipids in each leaflet. When 10% CHOL is included, $\Delta Z/2$ becomes slightly thicker and A decreases compared with pure PC bilayer systems. The mixed bilayers containing PODAG or SCER show similar structural properties (for instance, $\Delta Z/2 = 1.45$ nm and $A = 0.81$ nm^2 in PODAG/DAPC, $\Delta Z/2 = 1.45$ nm and $A = 0.81$ nm^2 in SCER/DAPC). Bilayers with PODAG or SCER show larger surface areas compared with those with CHOL, due to their larger molecular volumes.

We next investigated the orientation angles of CHOL, PODAG, and SCER in PC bilayers. The angle, θ, between the bilayer normal (z-axis) and the vector connecting head to tail group sites in CHOL

or that connecting the head group to center of mass in PODAG or SCER is used to define the orientation. The distribution of the orientation angles fitted a GAUSSIAN distribution function, so we list the maximum values as the most probable angle (Table 1). The DAPC, SAPC, and POPC bilayers have different unsaturation. CHOL is located near the membrane/water interfaces in all three lipid bilayers. In addition, CHOL is located near the bilayer center ($Z = 0$) only in DAPC (polyunsaturated) lipid bilayer as is shown by neutron-scattering experiments and recent CGMD simulations. In contrast, PODAG and SCER reside near the membrane/water interface in each leaflet ($\theta \approx 23°$ for PODAG/DAPC, $\theta \approx 21°$ for SCER/DAPC). As the number of unsaturated bonds in the acyl tails of PC is decreased, the orientation angles become smaller, suggesting a decrease in thermal fluctuations. PODAG tends to have larger orientation angles than SCER in all three membranes.

3.2. Flip-flop motions of DAG and CER in phospholipid bilayers

Figure 2 shows the motions of the hydroxyl head groups ($-OH$) of CHOL, PODAG, and SCER in three different PC lipid bilayers. As shown by Marrink et al. CHOL in a DAPC membrane exhibits fast flip-flop motions compared with those in SAPC and POPC membranes [18]. Our results on the flip-flop motions of CHOL over much longer simulations are consistent with theirs. We observed fast flip-flop motions of PODAG in DAPC bilayers, and slower flip-flop motions of PODAG in SAPC and SCER in DAPC bilayers. No flip-flop motions were observed for PODAG in POPC and SCER in SAPC and POPC bilayers within 80 μs-CGMD simulations. The rates for the flip-flop motions of CHOL, PODAG, and SCER followed the order of CHOL >> PODAG > SCER and the rates slowed as the number of unsaturated bonds in the PC decreased (DAPC > SAPC > POPC).

In experiments, flip-flop motions have been measured using fluorescent lipid analogs [13,14,42–46]. The transbilayer movement of NBD-PE has been measured in large unilamellar vesicles (LUV) of PC with varying acyl composition. The flip-flop rates of NBD-PE in PC membranes increase with the number of double bonds as follows, di16:0 PC < 18:0–18:1 PC < di18:1 PC < 18:0–18:2 PC < di18:2 PC < di18:3 PC < 18:0–22:6 PC [42]. The flip-flop motion of several types of lipids (PC, SM, CER, and DAG) has also been studied using DMB labeled analogs in LUVs [13], revealing much higher rates for DAG and CER than PC molecules. The half flip-flop time of DAG and CER were 70 ms and 22 min., respectively. To increase the accuracy of experimental measurements, we used the same fluorescent fatty acid, like C_{12}–NBD–PC, C_{12}–NBD–DAG and C_{12}–NBD–ceramide and measured their flip-flop motions in SUVs (final concentration 10 μM) with sodium dithionite (final concentration 10 mM) at 25 °C (Detailed experimental conditions are shown in Supporting Information). Those experiments show that (1) the flip-flop motions of C_{12}–NBD–DAG and C_{12}–NBD–ceramide were observed within an experimental time of 1000 s and (2) the intensity of C_{12}–NBD–ceramide decayed more slowly than that of C_{12}–NBD–DAG. This result suggests that the flip-flop rate increases in the order of CER < DAG.

In summary, experiments show that the flip-flop rate increases in the order of PC < SM < CER < DAG and that the rate also increases in unsaturated phospholipid bilayers. Experimental flip-flop times

Table 1
Structural properties of the mixed bilayers (bilayer thickness ($\Delta Z/2$) and area per lipid (A) for the bilayer systems and orientation angle (q) for CHOL, PODAG, or SCER) in the CGMD simulations.

	CHOL/DAPC	PODAG/DAPC	SCER/DAPC	CHOL/SAPC	PODAG/SAPC	SCER/SAPC	CHOL/POPC	PODAG/POPC	SCER/POPC
$\Delta Z/2$ (nm)	1.44	1.45	1.45	1.57	1.57	1.58	1.67	1.79	1.78
A (nm^2)	0.78	0.81	0.81	0.72	0.75	0.75	0.61	0.62	0.62
q (deg)	28 (90)[a]	23	21	24	20	18	18	17	16

[a] In the simulation of CHOL/DAPC, the bilayer center has a peak for the orientation angle of CHOL as well as at the membrane/water interfaces. In parenthesis, the most probable angle observed at the bilayer center is listed.
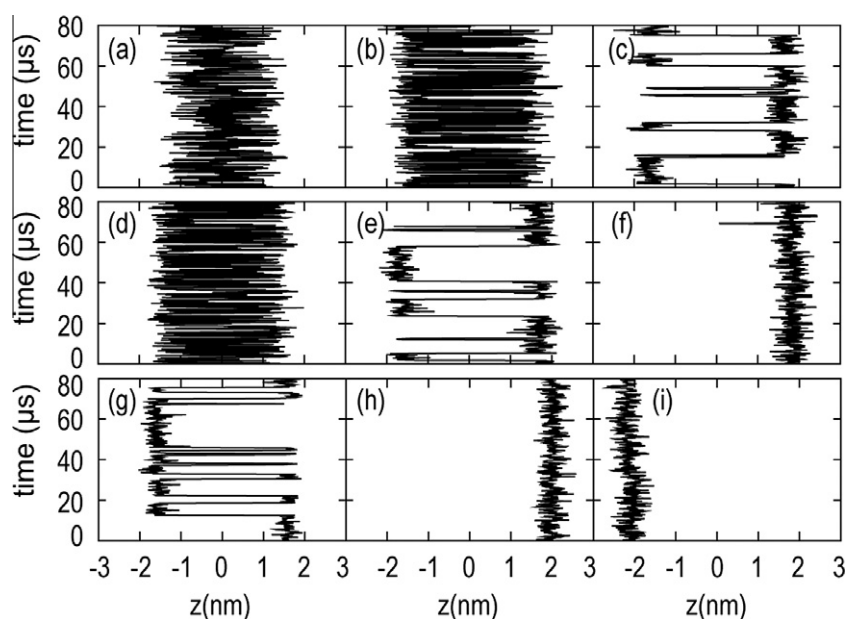
Figure 2. The motion of head groups in one CHOL, PODAG, and SCER along the bilayer normal in each simulation system ((a) CHOL/DAPC, (b) PODAG/DAPC, (c) SCER/DAPC, (d) CHOL/SAPC, (e) PODAG/SAPC, (f) SCER/SAPC, (g) CHOL/POPC, (h) PODAG/POPC, (i) SCER/POPC).

of CER and DAG are ms or longer, whereas we could observe the flip-flop motions of CER and DAG in 80 μs simulations. This apparent discrepancy could be mainly due to the difference of lipid-bilayer systems. In experiments, the PC lipids with few unsaturated bonds in their acyl chains are used due to the technical conveniences, whereas we used DAPC (di20:4 PC) or SAPC (18:0–20:4 PC) in CGMD and all-atom MD simulations to observe the flip-flop motions of CER and DAG in reasonable computational time. Actually, in POPC (16:0–18:1 PC) lipid bilayers, we could not observe any flip-flop motions of DAG and CER during 80 μs CGMD simulations. The usage of fluorescent lipid analog in experiment may decrease the flip-flop rates compared with those of natural DAG and CER. Therefore, although the direct comparison between the experiment and current simulations is difficult, the order of flip-flop rates for CHOL, CER, and DAG are the same as those obtained by experiments.

The orientation angles of CHOL, PODAG, and SCER are strongly correlated with their head-group positions along the bilayer normal (Figure 3). To obtain the flip-flop rates of CHOL, PODAG, and SCER more quantitatively, we studied a single flip-flop process as a jump between the two membrane/water interfaces. Because the distribution of head group positions is so broad, we used the orientation angle, θ, for defining the three states: S0 (membrane interior: $60° < \theta < 120$), S1 (a membrane interface: $0° < \theta < 60°$), and S1′ (another interface: $120° < \theta < 180°$). A flip-flop process is then counted when a lipid jumps from S1 to S1′ (or from S1′ to S1). In Table 2, we list the total number of flip-flop events, $N_{\text{flip-flop}}$, and the average flip-flop time, $t_{\text{flip-flop}}$, in 80 μs-CGMD simulations. Here, we define the average flip-flop time as the total simulation time divided by the number of flip-flop events in the simulation. Compared with CHOL, flip-flop rates for PODAG and SCER are 5.7 times and 235.0 times slower in the DAPC bilayer, respectively. Figure 4 shows a series of simulation snapshots of a flip-flop event of single molecules of CHOL, PODAG, and SCER in DAPC bilayers. The first frame ($t = 0$) is taken when the selected lipid just begins to jump between the two leaflets. Contrary to the large differences in the average flip-flop time, the time required for a jump is almost within the same time scale for CHOL, PODAG, and SCER.

3.3. Statistical analysis on the flip-flop events

We investigated the residence time of CHOL, PODAG, and SCER at S0 (membrane interior), S1, and S1′ (membrane interfaces). Figure 5 shows that the probability distributions for the residence time at S0 for CHOL, PODAG, and SCER are well-fitted to a single exponential curve, whereas different exponential curves are
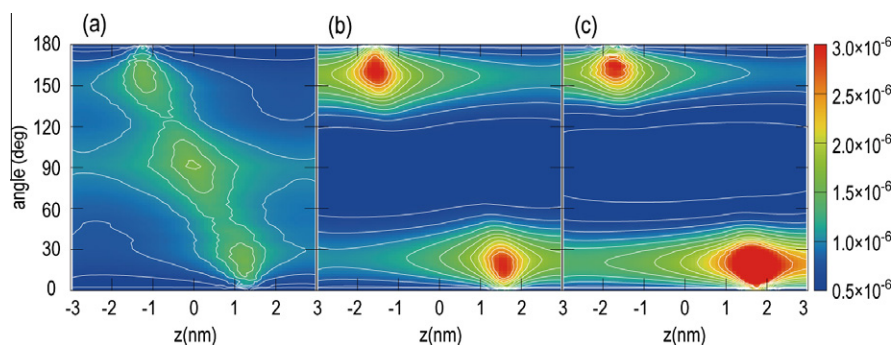
Figure 3. Distributions of the orientation angle and the head-group position along the bilayer normal for (a) CHOL, (b) PODAG, and (c) SCER in the DAPC bilayer. The white lines show counter lines in the distributions.

Table 2
The flip-flop time and average position of each chemical group in the CGMD simulations.

	CHOL/DAPC	PODAG/DAPC	SCER/DAPC	CHOL/SAPC	PODAG/SAPC	SCER/SAPC	CHOL/POPC	PODAG/POPC	SCER/POPC
$N_{flip\text{-}flop}$[a]	1821.25	318.5	7.75	266.0	12	–	34.25	–	–
$t_{flip\text{-}flop}$[b] (μs)	0.044	0.251	10.323	0.301	6.667	–	2.336	–	–
Z_{NC3}[c] (nm)	1.99	2.03	2.01	2.09	2.07	2.11	2.21	2.31	2.29
Z_{PO3}[d] (nm)	1.88	1.90	1.90	1.99	1.98	2.01	2.11	2.23	2.21
Z_{GL}[e] (nm)	1.44	1.46	1.45	1.57	1.57	1.58	1.67	1.79	1.78
Z_{OH}[f] (nm)	1.26	1.48	1.68	1.40	1.64	1.84	1.57	1.96	2.10

[a] The number of flip-flop events per single lipid molecule included in each 80 μs-simulation system was averaged and listed.
[b] Averaged flip-flop time per lipid.
[c–f] Average position of each chemical group ([c]choline, [d]phosphate, [e]glycerol backbone in PC, [f]OH in CHOL, PODAG, or SCER).
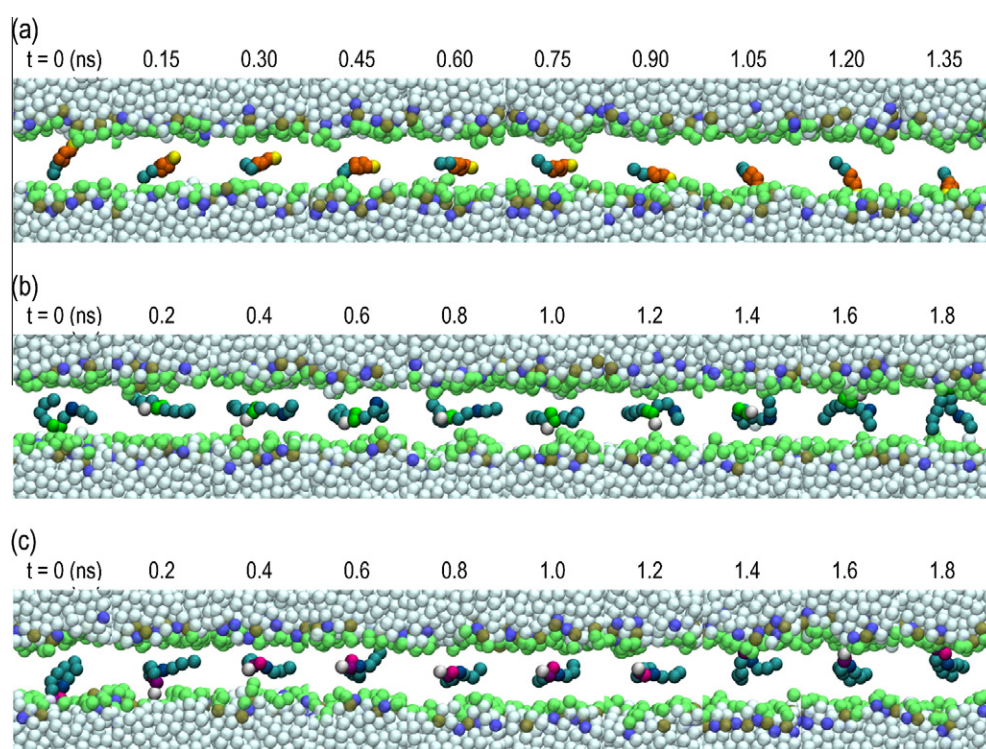
Figure 4. Selected snapshots in the simulations for (a) CHOL/DAPC, (b) PODAG/DAPC, and (c) SCER/DAPC. Only one flip-flop event is shown for each figure. The acyl chains of DAPC and other molecules of CHOL, PODAG, or SCER in each system are neglected for clarity. We set $t = 0$, when a lipid molecule starts to move from one of the leaflets to another. The choline, phosphate, and glycerol backbones in DAPC lipids are displayed. Particles colored in ocher, blue, and green represent choline, phosphate, and glycerol backbones in DAPC, respectively. White particles represent coarse-grained water.

required to fit the distributions at S1 and S1′ for the three lipid molecules. In order to gain further insights into the different situations, we devised a simple stochastic model as follows. First, we treat a transition between two different states as an independent stochastic event with constant rates, λ_0(S0 → S1 and S0 → S1′) and λ_1(S1 → S0 and S1′ → S0) per unit time. We consider a short time interval Δt during which a transition occurs once at most. Then, the probability for a transition event can be defined as $\lambda_i \Delta t$ ($i = 0, 1$). If we consider the case when a transition occurs after $n\Delta t$ times of attempted transitions, the probability can be written as $(1 - \lambda_i \Delta t)^n \lambda_i \Delta t$. Taking the limit for $\Delta t \to 0$ and $n \to \infty$, we obtain $P(t) = \lambda_i \exp(-\lambda_i t)$. The single exponential curve in Figure 5a suggests that the rate of transitions from the membrane interior, λ_0, is independent of the type of lipid molecule flipping, and hence independent of its interaction with phospholipids. Membrane fluidity appears to determine λ_0 rather than specific interactions with phospholipid molecules. Thus, it is more easily understood why flip-flop rates for these molecules correlate well with the number of unsaturated bonds in the phospholipid molecules. In contrast, the rate of transitions from the membrane interfaces, λ_1, differs

among CHOL, PODAG, and SCER, suggesting that each lipid interacts differently with the lipid molecules at the interfaces.

3.4. Hydration effect on the flip-flop motion

To examine interactions at the membrane/water interfaces in more detail, we carried out atomistic simulations for CHOL/DAPC, PODAG/DAPC, and SCER/DAPC. Figure 6 shows the snapshots of single molecules of CHOL, PODAG, and SCER and the density profiles of the glycerol backbone (GL) in DAPC, the head group (OH) in CHOL, PODAG, and SCER, and water for these systems. Due to limited sampling in these atomistic simulations, CHOL is trapped at one of the membrane/water interfaces, although it also exists in the interior of the membrane over longer CGMD simulations. PODAG and SCER also stay at one of the interfaces. However, the positions of the head groups of CHOL, PODAG, and SCER relative to GL in the phospholipid bilayer differ significantly. The head group of CHOL exists inside of GL, whereas that of SCER is located outside of GL, suggesting that there is stronger interaction between SCER and water molecules at the interfaces. The head group of
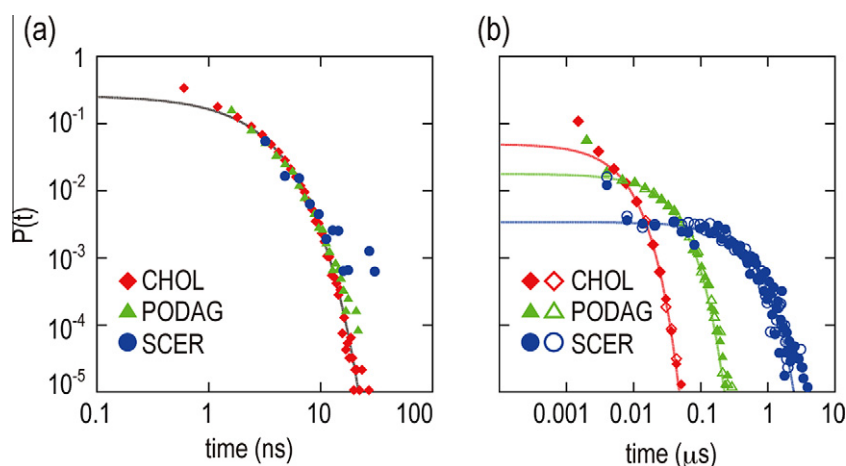
Figure 5. Probability densities for the residence time of CHOL (red), PODAG (green), and SCER (blue) at the interior (a) and DAPC-membrane/water interface (b). In Figure 5b, filled and open marks are the densities at the upper and lower interfaces of DAPC, respectively. The straight lines are exponential curves fitted to the probability densities.
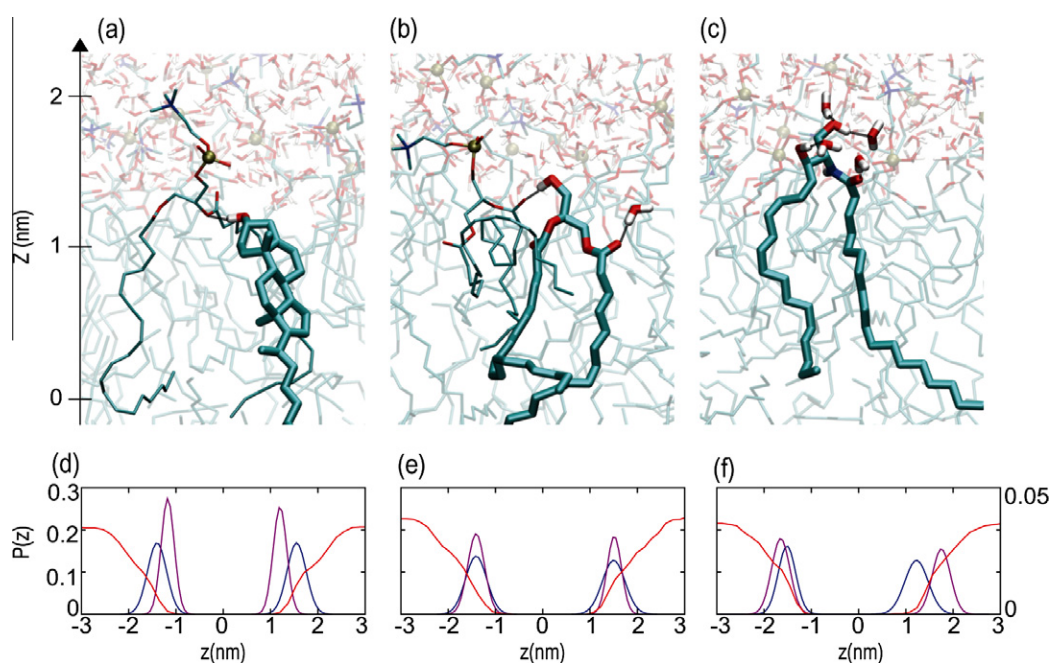
Figure 6. Snapshots and density profiles in atomistic MD simulations. One molecule of (a) CHOL, (b) PODAG, and (c) SCER is shown in stick model. Water molecules that form hydrogen bonds with these lipids are also shown in stick model. The density profiles of glycerol backbone in DAPC, head group (OH) in (d) CHOL, (e) PODAG, and (f) SCER, and water are shown in blue, purple, and red straight lines, respectively.

PODAG lies between CHOL and SCER. The structures of CHOL, PODAG, and SCER at the membrane water interfaces obtained in the final snapshot in each atomistic MD simulation agree with these results (Figure 6). Here CHOL does not hydrogen bond with water, PODAG bonds with one water molecule, and SCER with four. The atomistic simulations suggest that flip-flop rates correlate with head group hydration. This helps to explain why the flip-flop motions of PC and PE are so slow in comparison with PODAG and SCER – the phosphate group of the former greatly increases hydration. And why changing the hydroxyl group of CHOL to the less polar keto group of ketosterone increases flip-flops 1.5×10^3 fold [15,16].

By utilizing both CG and atomistic MD simulations, more insights are gained into the detailed mechanisms underlying flip-flop rates for different lipid molecules in PC bilayers. Such multi-scale simulation approaches should be useful for understanding other, rather slower biological events particularly those in the biological membranes.

4. Conclusion

We have investigated the flip-flop motions of PODAG and SCER in PC lipid bilayers using both coarse-grained and atomistic MD simulations. The rates of transbilayer movements of PODAG and SCER are much faster than those of phospholipids and the flip-flop of PODAG is faster than that of SCER. Although the flip-flop rates of naturally occurring DAG and CER are not known, published data of fluorescent DAG and CER analogs are consistent with our results. Moreover, the flip-flop rate depends on the physical condition of the membrane and the transverse lipid movement has different

rate in different membrane. When the number of double bond of the acyl tails of the bilayer lipid increases, the flip-flop rate significantly increases (DAPC > SAPC > POPC). In our simulations, the flip-flop events of CHOL, PODAG, and SCER were well described by a Poisson process and the order of their flip-flop rates reflected the difference of the residence times of transverse lipids at the membrane/water interfaces. Another prediction of our results is that the transbilayer movement of the lipids is also affected by the fatty acid composition of surrounding lipid molecules [47].

The type of flip-flop motion depends on the type of lipid molecule traversing the bilayer. Unlike in our simulations, Tieleman and Marrink et al. observed water permeation in concert with the flip-flop motion of PC lipid molecules using the umbrella sampling method [19]. A few water molecules bound to the PC accompany the lipid during the flip-flop process. We did not observe the formation of pores in the membranes during the flip-flop motions of CHOL, PODAG, and SCER. To examine the interaction between water and lipid molecules in detail, we also performed simulations of the same lipid systems using the polarizable MARTINI water model [28]. However we observed only minor differences in the rates, validating the current simulations (simulation results of the polarizable MARTINI water model are shown in Supporting Information).

CER plays a crucial role in divergent signaling events including differentiation, senescence, proliferation, and apoptosis [48–50]. On the plasma membrane, CER concentration is increased upon cell activation by the hydrolysis of sphingomyelin (SM), which is located in the outer leaflet of the plasma membrane. It is proposed that the accumulation of CER forms distinct lipid domains that provide a platform for various signaling event [11]. Our results suggest that CER formed on the outer leaflet of the plasma membrane are rapidly transported to the inner leaflet and the transbilayer distribution of CER is dependent on the physical properties of the surrounding lipids.

Acknowledgments

Appendix A. Supplementary data

Supplementary data associated with this article can be found, in the online version, at doi:10.1016/j.cplett.2011.11.057.

References

[1] A. Zachowski, Biochem. J. 294 (Pt 1) (1993) 1.
[2] A.A. Gurttovenko, J. Anwar, I. Vattulainen, Chem. Rev. 100 (2010) 6077.
[3] J.C.M. Holthuis, T.P. Levine, Nat. Rev. Mol. Cell Biol. 6 (2005) 209.
[4] F.X. Contreras, L.S. Magraner, A. Alonso, F.M. Goni, FEBS Lett. 584 (2010) 1779.
[5] G. van Meer, D. Voelker, G. Feigenson, Nat. Rev. Mol. Cell Biol. (2008) 112.
[6] C.L. Yen, S.J. Stone, S. Koliwad, C. Harris, R.V. Farese Jr., J. Lipid Res. 49 (2008) 2283.
[7] F.M. Goni, A. Alonso, Prog. Lipid Res. 38 (1999) 1.
[8] M.N. Hodgkin, T.R. Pettitt, A. Martin, R.H. Michell, A.J. Pemberton, M.J. Wakelam, Trends Biochem. Sci. 23 (1998) 200.
[9] M.J. Wakelam, Biochim. Biophys. Acta 1436 (1998) 117.
[10] A.H. Futerman, H. Riezman, Trends Cell Biol. 15 (2005) 312.
[11] K. Hanada, K. Kumagai, N. Tomishige, T. Yamaji, Biochim. Biophys. Acta 1791 (2009) 684.
[12] W.J. van Blitterswijk, A.H. van der Luit, R.J. Veldman, M. Verheij, J. Borst, Biochem. J. 369 (2003) 199.
[13] J.N. Bai, R.E. Pagano, Biochemistry 36 (1997) 8840.
[14] B.R. Ganong, R.M. Bell, Biochemistry 23 (1984) 4977.
[15] T. Rog, L.M. Stimson, M. Pasenkiewicz-Gierula, I. Vattulainen, M. Karttunen, J. Phys. Chem. B 112 (2008) 1946.
[16] W.F.D. Bennett, J.L. MacCallum, M.J. Hinner, S.J. Marrink, D.P. Tieleman, J. Am. Chem. Soc. 131 (2009) 12714.
[17] S. Jo, H. Rui, J. Lim, J. Klauda, W. Im, J. Phys. Chem. B 144 (2010) 13342.
[18] S.J. Marrink, A.H. de Vries, T.A. Harroun, J. Katsaras, S.R. Wassall, J. Am. Chem. Soc. 130 (2008) 10.
[19] D.P. Tieleman, S.J. Marrink, J. Am. Chem. Soc. 128 (2006) 12462.
[20] W.F.D. Bennett, J.L. MacCallum, D.P. Tieleman, J. Am. Chem. Soc. 131 (2009) 1972.
[21] N. Sapay, W.F.D. Bennett, D.P. Tieleman, Soft Matter 5 (2009) 3295.
[22] A.A. Gurtovenko, I. Vattulainen, J. Phys. Chem. B 111 (2007) 13554.
[23] S.J. Marrink, A.H. de Vries, A.E. Mark, J. Phys. Chem. B 108 (2004) 750.
[24] S.J. Marrink, H.J. Risselada, S. Yefimov, D.P. Tieleman, A.H. de Vries, J. Phys. Chem. B 111 (2007) 7812.
[25] H.J.C. Berendsen, D. Vanderspoel, R. Vandrunen, Comput. Phys. Commun. 91 (1995) 43.
[26] E. Lindahl, B. Hess, D. van der Spoel, J. Mol. Model. 7 (2001) 306.
[27] S.O. Yesylevskyy, L.V. Schäfer, D. Sengupta, S.J. Marrink, PLoS Comput. Biol. 6 (2010) e1000810.
[28] B. Hess, C. Kutzner, D. van der Spoel, E. Lindahl, J. Chem. Theory Comput. 4 (2008) 435.
[29] O. Berger, O. Edholm, F. Jahnig, Biophys. J. 72 (1997) 2002.
[30] M. Bachar, P. Brunelle, D.P. Tieleman, A. Rauk, J. Phys. Chem. B 108 (2004) 7170.
[31] M. Holtje, T. Forster, B. Brandt, T. Engels, W. von Rybinski, H.D. Holtje, Biochimica Et Biophysica Acta-Biomembranes 1511 (2001) 156.
[32] H.J.C. Berendsen, J.P.M. Postma, W.F. van Gunsteren, J.. Hermans, Interaction models for water in relation to protein hydration, in: D.B. Pullman (Ed.), Intermeclular Forces, D. Reidel Publishing Co., The Netherlands, 1981, pp. 331–342.
[33] S.W. Chiu, M.M. Clark, E. Jakobsson, S. Subramaniam, H.L. Scott, J. Phys. Chem. B 103 (1999) 6323.
[34] S.W. Chiu, S. Vasudevan, E. Jakobsson, R.J. Mashl, H.L. Scott, Biophys. J. 85 (2003) 3624.
[35] S.A. Pandit, H.L. Scott, J. Chem. Phys. 124 (2006).
[36] L. Monticelli, S.K. Kandasamy, X. Periole, R.G. Larson, D.P. Tieleman, S.J. Marrink, J. Chem. Theory Comput. 4 (2008) 819.
[37] T. Darden, D. York, L. Pedersen, J. Chem. Phys. 98 (1993) 10089.
[38] U. Essmann, L. Perera, M.L. Berkowitz, T. Darden, H. Lee, L.G. Pedersen, J. Chem. Phys. 103 (1995) 8577.
[39] B. Hess, H. Bekker, H.J.C. Berendsen, J. Fraaije, J. Comput. Chem. 18 (1997) 1463.
[40] S. Miyamoto, P.A. Kollman, J. Comput. Chem. 13 (1992) 952.
[41] H.J.C. Berendsen, J.P.M. Postma, W.F. Vangunsteren, A. Dinola, J.R. Haak, J. Chem. Phys. 81 (1984) 3684.
[42] V.T. Armstrong, M.R. Brzustowicz, S.R. Wassall, L.J. Jenski, W. Stillwell, Arch. Biochem. Biophys. 414 (2003) 74.
[43] I. Lopez-Montero, N. Rodriguez, S. Cribier, A. Pohl, M. Velez, P.F. Devaux, J. Biol. Chem. 280 (2005) 25811.
[44] A. Pohl, I. Lopez-Montero, F. Rouviere, F. Giusti, P.F. Devaux, Mol. Membr. Biol. 26 (2009) 194.
[45] J.A. Hamilton, Curr. Opin. Lipidol. 14 (2003) 263.
[46] F.X. Contreras, G. Basanez, A. Alonso, A. Herrmann, F.M. Goni, Biophys. J. 88 (2005) 348.
[47] L.M. Obeid, C.M. Linardic, L.A. Karolak, Y.A. Hannun, Science 259 (1993) 1769.
[48] T. Okazaki, R.M. Bell, Y.A. Hannun, J. Biol. Chem. 264 (1989) 19076.
[49] M.E. Venable, J.Y. Lee, M.J. Smyth, A. Bielawska, L.M. Obeid, J. Biol. Chem. 270 (1995) 30701.
[50] D. Adam, M. Heinrich, D. Kabelitz, S. Schutze, Trends Immunol. 23 (2002) 1.